



Highly accelerated compressed sensing time-of-flight magnetic resonance angiography may be reliable for diagnosing head and neck arterial steno-occlusive disease: a comparative study with digital subtraction angiography

Xuan Zhang¹ · Yue Zhou Cao¹ · Xi Hu Mu¹ · Yi Sun² · Michaela Schmidt³ · Christoph Forman³ · Peter Speier³ · Shan Shan Lu¹ · Xun Ning Hong¹

Received: 2 August 2019 / Revised: 10 December 2019 / Accepted: 28 January 2020 / Published online: 17 February 2020

© European Society of Radiology 2020

Abstract

Introduction We aimed to investigate the utility of compressed sensing time-of-flight magnetic resonance angiography (CS TOF-MRA) for diagnosing intracranial and cervical arterial stenosis by using digital subtraction angiography (DSA) as the reference standard.

Methods Thirty-seven patients with head and neck arterial stenoses who underwent CS TOF-MRA and DSA were retrospectively enrolled. The reconstructed resolution of CS TOF-MRA was $0.4 \times 0.4 \times 0.4 \text{ mm}^3$. The scan time was 5 min and 2 s. The image quality of CS TOF-MRA was independently ranked by two neuroradiologists in 1031 arterial segments. The luminal stenosis grades on CS TOF-MRA and DSA were analyzed in 61 arterial segments and were compared using the Wilcoxon signed-rank test. The ability of CS TOF-MRA to predict moderate to severe stenosis or occlusion was analyzed.

Results The image quality of most arterial segments (95.2%) on CS TOF-MRA was excellent. Arterial segments with low image quality were mainly the V3–4 segments of the vertebral artery. The majority of arterial stenoses (62.3%) were located in the cervical internal carotid artery. The luminal stenosis grades of CS TOF-MRA were concordant with that of DSA in 50 of 61 segments ($p = 0.366$). CS TOF-MRA had a sensitivity of 84.4% and a specificity of 88.5% for predicting moderate to severe stenosis. For detecting occlusion lesions, it had a sensitivity of 100% and a specificity of 94.1%.

Conclusion CS TOF-MRA provides adequate image quality within a reasonable acquisition time and is a reliable tool for diagnosing head and neck arterial steno-occlusive disease.

Xuan Zhang and Yue Zhou Cao contributed equally to this work.

Electronic supplementary material The online version of this article (<https://doi.org/10.1007/s00330-020-06682-3>) contains supplementary material, which is available to authorized users.

✉ Shan Shan Lu
lushan1118@163.com

✉ Xun Ning Hong
hongxunning@sina.com

¹ Department of Radiology, The First Affiliated Hospital of Nanjing Medical University, No. 300 Guangzhou Road, Gulou district, Nanjing, Jiangsu Province, China

² MR Collaboration, Siemens Healthcare Ltd., Shanghai, China

³ Siemens Healthcare GmbH, Erlangen, Germany

Key Points

- CS TOF-MRA provides a relatively large coverage (16 cm), high resolution ($0.4 \times 0.4 \times 0.4 \text{ mm}^3$) and good image quality of head and neck arteries within 5 min and 2 s.
- The diagnostic accuracy of CS TOF-MRA in the assessment of moderate to severe stenosis and occlusion was comparable with that of DSA.
- Arterial segments with low image quality were mainly the V3 and V4 segments of the vertebral artery.

Keywords Magnetic resonance angiography · Digital subtraction angiography · Stenosis

Abbreviations

ACA	Anterior cerebral artery
BA	Basilar artery
CS TOF-MRA	Compressed sensing time-of-flight magnetic resonance angiography
DSA	Digital subtraction angiography
ICA	Internal carotid artery
MCA	Middle cerebral artery
mFISTA	Modified fast iterative shrinkage-thresholding algorithm
NASCET	North American Symptomatic Carotid Endarterectomy Trial
PCA	Posterior cerebral artery
PI	Parallel imaging
SNR	Signal-to-noise ratio
VA	Vertebral artery
WASID	Warfarin Aspirin Symptomatic Intracranial Disease

Introduction

Stroke is a major cause of morbidity and mortality worldwide. Studies have found that intracranial and extracranial arterial atherosclerotic steno-occlusive disease is an important cause of ischemic stroke [1]. In this context, an accurate assessment of cerebral arteries is important for optimal therapeutic decisions. Digital subtraction angiography (DSA) is the gold standard for accessing vascular stenosis. However, DSA is an invasive, radiation-associated technique with the possibility of complications [2]. Currently, noninvasive techniques, such as three-dimensional time-of-flight magnetic resonance angiography (TOF-MRA), are widely used to evaluate and follow up patients with head and neck arterial disease and have been used to replace DSA in the diagnosis of cerebrovascular disease in clinical practice. TOF-MRA provides high contrast and spatial resolution. However, in order to achieve a compromise between high spatial resolution and acceptable scan time, the anatomical coverage is often limited [3]. Moreover, motion artifacts produced by swallowing, respiration, and neck movements are more likely to appear due to the long scan time

[4], which may reduce image quality and impair reader confidence in image diagnosis.

To shorten the acquisition time, undersampling strategies such as partial Fourier imaging and parallel imaging (PI) have been used [5]. These two methods omit phase encoding steps in a regular fashion. The acceleration achieved by these methods is limited by several factors. First, the acceleration factor is limited by the different encoding possibilities of the coils because of the resulting aliasing artifacts in the image domain. Second, reduced acquisition of energy in k-space reduces the available signal-to-noise ratio (SNR), and hence, PI can only be used when there is sufficient SNR in the original full-sampled image [6].

Recently, the application of methods based on compressed sensing (CS) theory has had a significant impact on the field of magnetic resonance imaging (MRI). CS is based on the principle that incoherent artifacts can be corrected by the spatial and temporal redundancy of MRI when k-space is undersampled by a random sampling mode [7]. Compared with conventional approaches, CS allows rapid acquisition of images by using fewer k-space samples [8]. When the sparsity increases, CS provides better accelerated acquisition for the transformed sparse domain. As angiograms are sparse in pixel domain, they are suitable for CS reconstruction. Milles et al quantitatively evaluated the performance of CS techniques for TOF-MRA and found that CS reconstruction outperforms traditional methods of undersampling [7]. Li et al proposed a CS-based 3D MRA sequence which provides excellent visualizations for carotid vessels and calcification in a short scan time [9]. Fushimi et al applied CS to data from cerebral aneurysms and evaluated the diagnostic quality of CS TOF-MRA [10]. Their results showed that most cerebral aneurysms were sufficiently recognized in CS TOF-MRA. Our previous study found that CS TOF-MRA could remarkably reduce the scan time and provide comparable image quality to PI TOF-MRA for diagnosing intracranial arterial stenoses [11]. However, the diagnostic performance of CS TOF-MRA for assessment of intracranial and cervical arterial stenosis has not yet been evaluated.

In this study, we investigated the utility of CS TOF-MRA for diagnosing intracranial and cervical arterial stenosis in a clinical setting by using digital subtraction angiography (DSA) as the reference standard.

Material and methods

Patients

This study was reviewed and approved by our Institutional Review Board. The need for patient consent was also waived by the same Institutional Review Board. From December 2017 to October 2018, 66 consecutive patients were retrospectively recruited in our single center according to the following criteria: (1) both intracranial and cervical CS TOF-MRA and DSA were performed; (2) at least one segment of head and neck arterial stenosis was confirmed on DSA; and (3) the time interval between CS TOF-MRA and DSA was less than 2 weeks. Patients who met the following criteria were excluded from further analysis: (1) patients diagnosed with non-atherosclerotic diseases like Moyamoya disease, dissection, or vasculitis ($n = 8$); (2) stent implantation had been performed in the interval between DSA and CS TOF-MRA ($n = 18$); and (3) patients with obvious motion artifacts on CS TOF-MRA ($n = 3$). Ultimately, a total of 37 patients were recruited. During the admission period, these patients were treated by angioplasty and stent placement ($n = 32$), interventional embolectomy ($n = 2$), or antiplatelet or anti-coagulant medication ($n = 3$).

MR angiography parameters

CS TOF-MRA was performed based on a research sequence and reconstruction prototype on a MAGNETOM Skyra 3-T MR scanner (Siemens Healthcare) with a 20-channel head/neck coil. The slice orientation was axial. The parameters were as follows: repetition time (TR) 21 ms, echo time (TE) 3.49 ms, flip angle 18° , field-of-view (FOV) $220 \times 200 \text{ mm}^2$, matrix 368×334 , slice thickness 0.4 mm, and number of slabs 8. The acquired resolution was $0.6 \times 0.6 \times 0.6 \text{ mm}^3$ and reconstructed to $0.4 \times 0.4 \times 0.4 \text{ mm}^3$, and the acceleration factor of CS TOF-MRA was set at 10.3. Neither phase nor slice partial Fourier was used. The scan range extended from the bifurcation of the common carotid artery to the body of the corpus callosum. Data were reconstructed using 10 iterations of the modified fast iterative shrinkage-thresholding algorithm (mFISTA) [12]. The source images of CS TOF-MRA were reconstructed with maximum intensity projection (MIP). Multiple 3-dimensional MIP images that were radially projected at 15° increments (rotation about the 3 orthogonal axes of the head) were generated. Moreover, 22 thin-slab (10 mm) MIP images were also reconstructed in coronal and sagittal views, respectively.

Digital subtraction angiography protocol

DSA was performed using the modified Seldinger method with a DSA machine (Philips Allura Xper FD20). A 5-French headhunter catheter was introduced into the ascending

aorta via the transfemoral route and navigated into the appropriate carotid or vertebral artery, as decided by the angiographer. The arteries were displayed in at least 2 projections by automatic injection of 6–8 mL of iodixanol 320 (Visipaque, GE Healthcare). DSA was performed with a 270-mm field of view and a 1024 matrix, yielding a measured pixel size of $0.27 \times 0.27 \text{ mm}^2$.

Imaging evaluation

We used MIP images of CS TOF-MRA for image analysis and source images as an assistant. MIP images were assessed independently in a randomized order by two neuroradiologists (X.Z. and S.S.L. with 4 and 6 years of experience, respectively) who were blinded to the results of DSA. The assessed segments of intracranial and cervical arteries were as follows: (1) internal carotid artery (ICA): cervical segment (C1), petrous segment (C2), lacerum segment (C3), cavernous segment (C4), anterior clinoid process segment, and ophthalmic and communicating segment (C5–7); (2) middle cerebral artery (MCA): horizontal segment (M1) and insular segment (M2); (3) anterior cerebral artery (ACA): the horizontal segment (A1) and the vertical segment (A2); (4) posterior cerebral artery (PCA): precommunicating segment (P1) and ambient segment (P2). Fetal PCA was also divided into P1 and P2 segments by taking the ventral surface of the brain stem as the boundary; (5) basilar artery (BA); (6) vertebral artery (VA): foraminal segment (V2), extraspinal segment (V3), and intradural segment (V4). The quality of the images was evaluated on a 3-point scale. Grade-1 images had heavily blurred vessel margins with severe image artifacts and poor image quality which could not be used for clinical evaluation. Grade-2 images had slightly obscured vessel margins with minor artifacts but an overall good image quality. Grade-3 images had no apparent image artifacts and had clear and sharp vessel margins with excellent image quality. To resolve any disagreement between the 2 readers, another senior neuroradiologist (X.N.H. with 20 years of experience) re-evaluated the images and assisted in reaching a consensus agreement. The consensus scores were used for the subsequent analyses.

The luminal stenosis ratios on CS TOF-MRA were calculated by two neuroradiologists (X.Z. and S.S.L. with 4 and 6 years of experience, respectively) in a randomized order. For analysis of DSA, one neurointerventional radiologist (Y.Z.C. with 12 years of experience) measured the luminal stenosis ratios without knowledge of the MRA results. The luminal stenosis ratio of intracranial arteries was calculated as follows: stenosis ratio (%) = $(1, \text{ narrow lumen diameter} / \text{reference lumen diameter}) \times 100\%$, according to the Warfarin Aspirin Symptomatic Intracranial Disease (WASID) criterion. The reference lumen was defined as the neighboring segment of normal appearance proximal to the stenotic site. The North

American Symptomatic Carotid Endarterectomy Trial (NASCET) method was used for calculating extracranial arterial stenosis ratio [13] as follows: stenosis ratio (%) = (1, artery diameter at the most narrow site/normal vessel diameter at the distal end of stenosis) × 100%. If there were multiple stenoses in one segment, only the most stenotic site would be selected for calculation. All stenoses were divided into 4 grades: grade 1, mild stenosis (0% < stenosis ratio < 50%); grade 2, moderate stenosis (50% ≤ stenosis ratio < 70%); grade 3, severe stenosis (70% ≤ stenosis ratio < 100%); and grade 4, occlusion, localized blood flow signals were lost, and the arterial wall was not shown.

Statistical analysis

All raw data were analyzed statistically using SPSS 22.0 (IBM Corporation; formerly SPSS Inc.). Intraclass correlation coefficient (ICC) was calculated to quantify the inter-observer reproducibility for stenosis assessment. The inter-observer reproducibility for image quality grading was performed using Cohen's kappa statistics. Reproducibility < 0.4 was characterized as poor, those 0.4–0.75 were fair to good, and those > 0.75 were considered excellent. The luminal stenosis ratio and stenosis grades on CS TOF-MRA and DSA were compared using the Wilcoxon signed-rank test. The sensitivity, specificity, positive predictive value (PPV), and negative predictive value (NPV) were calculated to analyze the diagnostic performance of CS TOF-MRA to predict moderate to severe stenosis (50–99% stenosis) and occlusion. The *p* value was two-sided, and *p* < 0.05 was considered statistically significant.

Results

Patient characteristic

A total of 1064 arterial segments of 37 patients (age, 64.3 ± 11.6; 26 males and 11 females) were included, of which 4 segments were excluded because of an inadequate scan range of CS TOF-MRA. In the remaining 1060 segments, 29 segments located after an occlusion with complete signal loss were excluded from the subsequent evaluation of image quality. Finally, 1031 segments were included for image quality assessment, of which 61 arterial segments with stenosis/occlusion were confirmed by DSA (Supplementary Table S1).

Acquisition time and image quality of CS TOF-MRA

The total scan time of CS TOF-MRA was 5 min and 2 s. The reconstruction time was 4 min and 14 s.

The inter-observer agreement for image quality grading was 0.816 (95% confidence interval 0.732, 0.900). The image quality of the majority of arterial segments on CS TOF-MRA

(95.2%) was graded as grade 3. The image quality of four segments (0.4%) was graded as grade 1 and 45 segments (4.4%) were graded as grade 2. The arterial segments with low image quality score were mainly vertebral artery V3 and V4 segments (detailed in Supplementary Table S2). Complete signal loss was observed in V2–V3 segments and V3–V4 segments of the left VA in two patients, and the image quality was scored as grade 1. The signal loss in these segments was eventually considered artifactual rather than true stenosis by the senior neuroradiologist, a determination which was verified by DSA (a representative case is shown in Supplementary Figure S1). These segments were excluded from the subsequent assessment of luminal stenosis.

Comparison between CS TOF-MRA and DSA for stenosis evaluation

The inter-observer agreement for stenosis assessment was 0.956 (95% confidence interval 0.928, 0.973). Detailed comparisons between CS TOF-MRA and DSA for evaluating intracranial and cervical arterial stenosis are summarized in Table 1 and Supplementary Tables S3. The luminal stenosis ratios measured on CS TOF-MRA were higher than those measured on DSA, but significant differences were only found in mild stenosis (Supplementary Table S3). The luminal stenosis grade of CS TOF-MRA was concordant with that of DSA in 50 of 61 segments (82.0%, Table 1). No significant differences between the luminal stenosis grades assessed on CS TOF-MRA and DSA were found according to the Wilcoxon signed-rank test (*p* = 0.366). Of the remaining 11 segments, 7 segments were overestimated and 4 segments were underestimated. Detailed results of those segments are summarized in Table 2. A representative case is shown in Fig. 1. (Several mismatched cases are presented in Supplementary Figures S2 to S5.)

The CS TOF-MRA had a sensitivity of 84.4%, a specificity of 88.5%, a PPV of 90%, and an NPV of 82.1% for predicting moderate to severe stenosis. For detecting occlusion lesions, CS TOF-MRA had a sensitivity of 100%, a specificity of 94.1%, a PPV of 76.9%, and an NPV of 100%.

Discussion

We evaluated the clinical value of CS TOF-MRA in the diagnosis of intracranial and cervical arterial stenosis by using digital subtraction angiography as the reference standard. We observed that CS TOF-MRA could provide good image quality and good agreement with DSA in the assessment of intracranial and cervical arterial stenosis in a reasonable acquisition time.

In this current study, the scan time of CS TOF-MRA for achieving a high-resolution in-plane resolution (0.4 ×

Table 1 Comparison of luminal stenosis grades between CS TOF-MRA and DSA

CS TOF-MRA	DSA			
	Mild stenosis	Moderate stenosis	Severe stenosis	Occlusion
Mild stenosis	13	2	0	0
Moderate stenosis	3	18	2	0
Severe stenosis	0	1	9	0
Occlusion	0	0	3	10

0.4 mm²) and a large anatomical range (16 cm) was 5 min and 2 s. We used a graphic processing unit (GPU), and the total reconstruction time after the scanning of CS TOF-MRA was 4 min and 14 s. This compares favorably to a conventional head and neck PI TOF-MRA (GRAPPA, 2; phase and slice partial Fourier, 7/8) which takes 18 min and 59 s using equivalent resolution and coverage to CS TOF-MRA; thus, the acquisition time was significantly reduced.

We evaluated the image quality of CS TOF-MRA for diagnosing intracranial and cervical stenosis. The orifice of the vertebral arteries was not included in the scan volume. The image quality of the majority of arterial segments on CS TOF-MRA was excellent. Artifacts were most commonly observed near the skull base, especially in V3 and V4 segments of vertebral arteries and in vessels near the sphenoid sinus. Such artifacts may lead to the false-positive diagnosis of arterial stenosis. Arteries near the skull base are subject to artifactual narrowing because of large susceptibility gradients present in this area [14]. Choi et al proposed that a smaller voxel size and a higher bandwidth may reduce this kind of artifact [15]. Another reason is that TOF-MRA is a gradient-echo technique in which contrast is obtained with unsaturated blood inflowing into a region of saturated stationary tissue [16]. It

has limitations for the assessment of slow-flowing blood. The vertebral artery is a common site of hypoplasia in arteries; thus, the slower blood flow through the narrower side of the vertebral artery can cause artifacts.

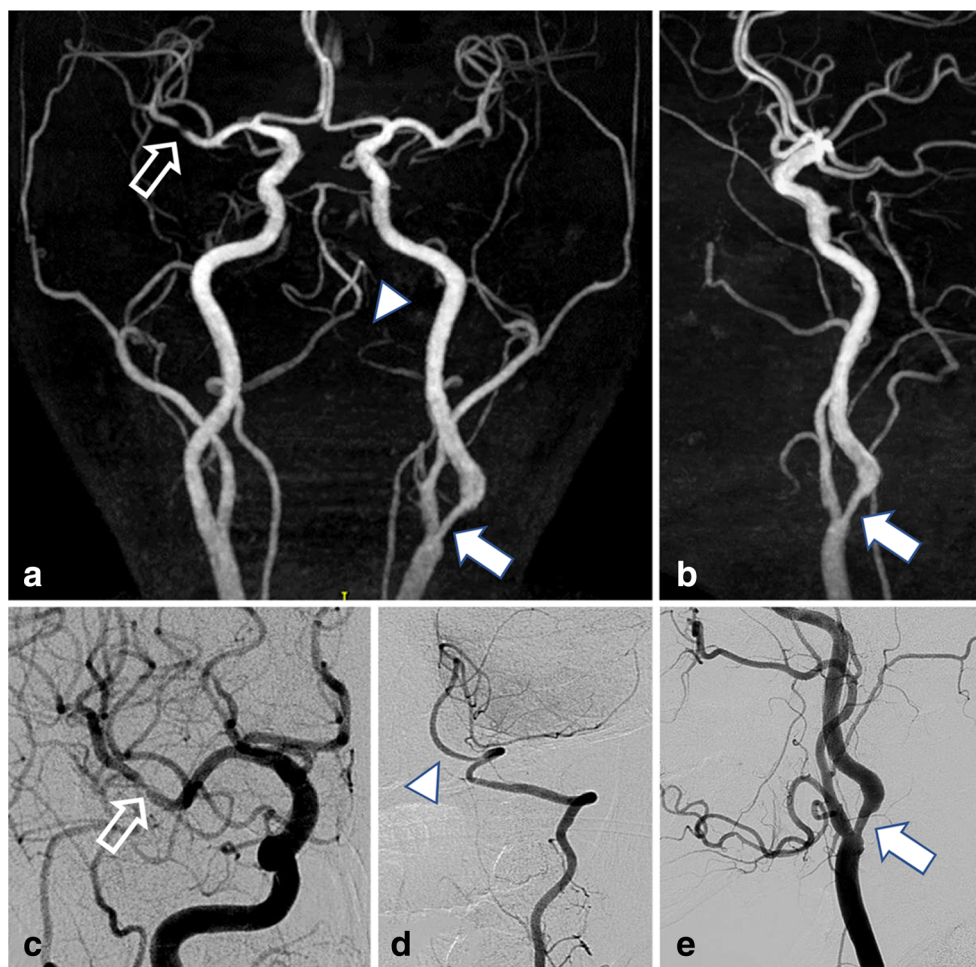
Previous studies that compared 3D TOF-MRA with DSA have reported that MRA tends to overestimate the degree of stenosis [17–19]. Our statistical results showed that there were no significant differences between the luminal stenosis grades assessed on CS TOF-MRA versus DSA. However, CS TOF-MRA tends to produce an overestimate when it is applied specifically to the luminal stenosis ratio. There are several possible reasons for this overestimation: (1) CS TOF-MRA may overestimate the actual stenosis rate. Accelerated flow through the stenotic site may lead to dephasing and overestimation of the extent of stenosis. Blood flow turbulence that occurs at the areas of bifurcation is believed to result in a loss of blood flow signal, because blood flow at different velocities with different phases tends to cancel each other [14]. This kind of artifact was one important source of stenotic overestimation in this study; (2) it is possible that DSA underestimates stenosis rather than MRA overestimates the extent of stenosis in some cases. According to a previous study, DSA does not always reveal the narrowest residual lumen because of the

Table 2 Summary of overestimated and underestimated segments by CS TOF-MRA

	Location	Stenosis on MRA (%)	Stenosis on DSA (%)	Estimated causes
Overestimated	LMCA M1	57	48	Borderline stenosis
	RMCA M1	59	47	Intra-voxel phase dispersion
	RACA A1	59	47	Borderline stenosis
	RICA C1	75	69	Borderline stenosis
	RICA C1	100	89	Near occlusion of proximal ICA without distal stenosis
	RICA C1	100	85	Near occlusion of proximal ICA without distal stenosis
Underestimated	RICA C1	100	84	Near occlusion of proximal ICA without distal stenosis
	LICA C1	63	80	Observer error
	RACA A2	63	76	Observer error
	RMCA M1	48	50	Borderline stenosis
	RICA C3	36	50	Borderline stenosis

LICA left internal carotid artery, RICA right internal carotid artery, LMCA left middle cerebral artery, RMCA right middle cerebral artery, RACA right anterior cerebral artery, LCCA left common carotid artery

Fig. 1 Compressed sensing time-of-flight MR angiography (CS TOF-MRA) and DSA in a 53-year-old patient. CS TOF-MRA shows a focal high-grade stenosis in the proximal M2 segment of the right middle cerebral artery with visible distal branches (**a**, hollow white arrow), and a focal high-grade stenosis in the proximal internal carotid artery (**a**, **b**; white arrow). DSA reveals almost identical features of stenosis (white hollow arrow in **c**, and white arrow in **e**) at the corresponding locations. Signal loss along the distal segment of the left vertebral artery is observed in CS TOF-MRA (**a**, white arrow head). DSA shows a left hypoplastic vertebral artery without any stenosis (**d**, white arrow head)



limited number of projections [20], which may lead to an underestimate of arterial stenosis. We also found that the stenosis of four segments was underestimated on CS TOF-MRA. In the present study, the main reason is the unavoidable measurement error when borderline stenosis occurs. Huston et al proposed that plaques with high signals on T1 might cause a high signal on MIP, thus masking signal loss on MIP display images [21]. This may be another reason for the underestimation of stenosis using CS TOF-MRA.

The diagnostic performance of CS TOF-MRA for detecting complete occlusion was excellent, with a sensitivity of 100%, a specificity of 94.1%, a PPV of 76.9%, and an NPV of 100%. In this current study, we considered discontinuity of flow on MIP images as occlusion. We found that this was the most common cause of overestimating severe stenosis as occlusion. Sadikin et al subdivided discontinuity into two parts, the gap sign and occlusion [18], and considered the gap sign as 99% stenosis rather than occlusion [22]. They demonstrated that the gap sign was more reliable in large arteries such as MCA, for depicting severe stenosis. If we subdivided the discontinuity in the same manner,

then the specificity of CS TOF-MRA may be improved. In predicting moderate to severe stenosis, CS TOF-MRA had a sensitivity of 84.4%, a specificity of 88.5%, a PPV of 90%, and an NPV of 82.1%. These results were comparable with those of previous studies [15, 18].

There were several limitations to our study. First, it was a retrospective study involving a relatively small number of stenotic arterial segments, 61. But we consider the total number of arterial segments, 1031, is sufficient for evaluating the image quality using CS TOF-MRA. Second, 38 of 61 arterial stenoses (62.3%) were located in the C1 segment of ICA. Other stenotic segments distributed nonhomogeneous. Thus, selection bias may have been introduced. However, in clinical settings, patients with mild or moderate intracranial arterial stenosis usually do not undergo DSA examinations, whereas many patients with severe proximal ICA stenosis would be treated with angioplasty and stent placement by DSA. Studies with a larger patient cohort including more stenoses in intracranial arteries and the first part of the vertebral arteries would strengthen the statistical power for the comparison between CS TOF-MRA and DSA in the future.

Conclusions

By combining 3D TOF-MRA with compressed sensing technology, a relatively large coverage (16 cm) of head and neck arteries with good image quality can be maintained within a reasonable acquisition time. In this study, the diagnostic accuracy of CS TOF-MRA was comparable with that of DSA in the assessment of moderate to severe stenosis and occlusion.

Funding information This study has not received any funding.

Compliance with ethical standards

Guarantor The scientific guarantor of this publication is Xun Ning Hong.

Conflict of interest Authors Yi Sun, Michaela Schmidt, Christoph Forman, and Peter Speier are employees of Siemens Healthcare. The remaining authors of this manuscript declare no relationships with any companies whose products or services may be related to the subject matter of the article.

Statistics and biometry No complex statistical methods were necessary for this paper.

Informed consent Written informed consent was waived by the Institutional Review Board.

Ethical approval Institutional Review Board approval was obtained.

Methodology

- Retrospective
- Performed at one institution

References

1. Johnston SC, Mendis S, Mathers CD (2009) Global variation in stroke burden and mortality: estimates from monitoring, surveillance, and modelling. *Lancet Neurol* 8:345–354
2. Willinsky RA, Taylor SM, Terbrugge K, Farb RI, Tomlinson G, Montanera W (2003) Neurologic complications of cerebral angiography: prospective analysis of 2,899 procedures and review of the literature. *Radiology* 227:522–528
3. Patel MR, Klufas RA, Kim D, Edelman RR, Kent KC (1994) MR angiography of the carotid bifurcation: artifacts and limitations. *AJR Am J Roentgenol* 162:1431–1437
4. Bousset L, Herigault G, de la Vega A, Nonent M, Douek PC, Serfaty JM (2006) Swallowing, arterial pulsation, and breathing induce motion artifacts in carotid artery MRI. *J Magn Reson Imaging* 23:413–415
5. Larkman DJ, Nunes RG (2007) Parallel magnetic resonance imaging. *Phys Med Biol* 52:R15–R55
6. Hollingsworth K (2015) Reducing acquisition time in clinical MRI by data undersampling and compressed sensing reconstruction. *Phys Med Biol* 60:R297–R322
7. Milles J, Versluis JM, Webb A, Reiber J (2010) Quantitative evaluation of compressed sensing in MRI: application to 7T time-of-flight angiography. Proceedings of the 10th IEEE International Conference on Information Technology and Applications in Biomedicine, Corfu, 2010, pp. 1–4
8. Lustig M, Donoho D, Pauly JM (2007) Sparse MRI: the application of compressed sensing for rapid MR imaging. *Magn Reson Med* 58:1182–1195
9. Li B, Li H, Dong L, Huang G (2017) Fast carotid artery MR angiography with compressed sensing based three-dimensional time-of-flight sequence. *Magn Reson Imaging* 43:129–135
10. Fushimi Y, Fujimoto K, Okada T et al (2016) Compressed sensing 3-dimensional time-of-flight magnetic resonance angiography for cerebral aneurysms: optimization and evaluation. *Invest Radiol* 51:228–235
11. Lu SS, Qi M, Zhang X et al (2018) Clinical evaluation of highly accelerated compressed sensing time-of-flight MR angiography for intracranial arterial stenosis. *AJNR Am J Neuroradiol* 39:1833–1838
12. Beck A, Teboulle M (2009) A fast iterative shrinkage-Thresholding algorithm for linear inverse problems. *SIAM J Imaging Sci* 2:183–202
13. (1991) North American Symptomatic Carotid Endarterectomy Trial. Methods, patient characteristics, and progress. *Stroke* 22:711–720. <https://doi.org/10.1161/01.STR.22.6.711>
14. Anderson CM, Saloner D, Tsuruda JS, Shapeero LG, Lee RE (1990) Artifacts in maximum-intensity-projection display of MR angiograms. *AJR Am J Roentgenol* 154:623–629
15. Choi CG, Lee DH, Lee JH et al (2007) Detection of intracranial atherosclerotic steno-occlusive disease with 3D time-of-flight magnetic resonance angiography with sensitivity encoding at 3T. *AJNR Am J Neuroradiol* 28:439–446
16. Nederkoom PJ, van der Graaf Y, Eikelboom BC, van der Lugt A, Bartels LW, Mali WP (2002) Time-of-flight MR angiography of carotid artery stenosis: does a flow void represent severe stenosis? *AJNR Am J Neuroradiol* 23:1779–1784
17. Serfaty JM, Chirossel P, Chevallerier JM, Ecochard R, Froment JC, Douek PC (2000) Accuracy of three-dimensional gadolinium-enhanced MR angiography in the assessment of extracranial carotid artery disease. *AJR Am J Roentgenol* 175:455–463
18. Sadikin C, Teng MM, Chen TY et al (2007) The current role of 1.5T non-contrast 3D time-of-flight magnetic resonance angiography to detect intracranial steno-occlusive disease. *J Formos Med Assoc* 106:691–699
19. Hirai T, Korogi Y, Ono K et al (2002) Prospective evaluation of suspected stenocclusive disease of the intracranial artery: combined MR angiography and CT angiography compared with digital subtraction angiography. *AJNR Am J Neuroradiol* 23:93–101
20. Nederkoom PJ, Elgersma OE, Mali WP, Eikelboom BC, Kappelle LJ, van der Graaf Y (2002) Overestimation of carotid artery stenosis with magnetic resonance angiography compared with digital subtraction angiography. *J Vasc Surg* 36:806–813
21. Huston J 3rd, Lewis BD, Wiebers DO, Meyer FB, Riederer SJ, Weaver AL (1993) Carotid artery: prospective blinded comparison of two-dimensional time-of-flight MR angiography with conventional angiography and duplex US. *Radiology* 186:339–344
22. Samuels OB, Joseph GJ, Lynn MJ, Smith HA, Chimowitz MI (2000) A standardized method for measuring intracranial arterial stenosis. *AJNR Am J Neuroradiol* 21:643–646

Publisher's note Springer Nature remains neutral with regard to jurisdictional claims in published maps and institutional affiliations.